VIROLOGY 219, 465–470 (1996)
ARTICLE NO. 0272

SHORT COMMUNICATION

Rod-Like Shape of Vesicular Stomatitis Virus Matrix Protein

ANNIE BARGE,* JEAN GAGNON,† ALAIN CHAFFOTTE,‡ PETER TIMMINS,§ JÖRG LANGOWSKI,*,[1]
ROB W. H. RUIGROK,* and YVES GAUDIN[¶,2]

*EMBL Grenoble Outstation, c/o ILL, BP 156, 38042 Grenoble Cedex 9, France; †Institut de Biologie Structurale, CEA/CNRS, 41 Avenue des Martyrs, 38027 Grenoble Cedex 1, France; ‡Institut Pasteur, Unité de Biochimie Cellulaire, 28 rue du Docteur Roux, 75724 Paris Cedex 15, France; §Institut Laue Langevin, BP 156, 38042 Grenoble Cedex 9, France; and ¶Laboratoire de Génétique des virus, CNRS, 91198 Gif sur Yvette Cedex, France

Received December 7, 1995; accepted March 19, 1996

The shape of purified matrix protein (M) of vesicular stomatitis virus was determined using biophysical techniques like analytical centrifugation, dynamic light scattering, and small-angle neutron scattering. The data obtained are consistent with a rod-like model for M protein with a length of about 100 ± 10 Å and a radius of 9 ± 1 Å. These dimensions are in agreement with the substructure of M protein aggregates and with the fine morphology of the axial channel material found inside the viral nucleocapsid coil. This morphological information was combined with CD measurements and secondary structure predictions on four vesiculovirus M proteins leading to a proposal for the structure of M protein.

The matrix protein of vesicular stomatitis virus (VSV M protein: 229 aa, 26.1 kDa) is the most abundant protein of the virus. During the viral cycle, M protein acts as a multifunctional protein. It plays a central role in viral assembly and budding (see below) but it has also been shown to inhibit the transcription of the viral genome both *in vitro* and *in vivo* (*1–4*) and to be directly involved in some of the VSV cytopathic effects (*5, 6*) and in virus-induced inhibition of transcription of host genes (*7, 8*).

In infected cells, part of the matrix protein population is stably associated with the plasma membrane (*9–12*). This population (about 10% of total M protein) has the characteristics of an integral membrane protein (*10, 11*), whereas most of the cellular M protein is found soluble in the cytoplasm (*10, 11, 13*) up to the moment of incorporation into new virions (*14*).

Concerning the position and structural role of VSV M protein inside the virion two different views prevail. Everyone agrees on the idea that M protein can condense the viral nucleocapsid (RNA encapsidated by the nucleoprotein) into a tightly coiled helical structure called the skeleton (*2, 15–18*). However, the question remains whether M is positioned outside the skeleton or inside. The generally accepted view is that M is positioned on the outside of the skeleton and acts as a bridge between the nucleocapsid coil and the viral membrane (*19–21*). As a second possibility we have suggested that the M protein may form a kind of scaffold around which the nucleocapsid is wound (*18*), in agreement with a model previously proposed by Brown and Newcomb (*22*) and with the results of Odenwald *et al.* (*17*). However, our results did suggest an interaction between M and membrane lipids at the extreme ends of the skeleton since we observed binding of negatively charged liposomes to the ends of the skeletons in electron microscopy (*18*). This interaction may be mediated by the highly basic amino-terminal region of the M protein which has been suggested to penetrate the viral membrane (*23*).

A protocol of purification of the matrix protein from the virion has been developed (*13, 24*). Purified M protein is soluble and monomeric in the absence of detergent at high salt concentrations. At low salt concentrations, aggregates are formed which share common morphological aspects with the M structure proposed to be inside the nucleocapsids (*18, 24*). We have suggested that this aggregation at low salt concentrations reflects the ability of M to self-associate to form this internal scaffold. We have also described conditions where the M protein remains soluble even at low salt concentrations, indicating that M protein purified from the virion behaves as a soluble cytoplasmic protein (*24*).

Although there is an increasing amount of information on the functions of negative-strand virus matrix proteins,

[1] Present address: DKFZ, Abteilung Biophysik der Makromoleküle, Im Neuenheimer Feld, D-69120 Heidelberg, Germany.

[2] To whom correspondence and reprint requests should be addressed. Fax: +33-1-69-82-43-08; E-mail: Yves.Gaudin@cnrs-gif.fr.

0042-6822/96 $18.00

very little is known about their structures. Crystallization trials of VSV M protein have so far been unsuccessful (Y. Gaudin and M. Knossow, unpublished results) and, therefore, we decided to determine the overall shape of M protein using various biophysical techniques.

M protein of VSV (Indiana Orsay strain) was isolated as previously described (*24*). All biophysical studies (except circular dichroism measurements, see below) were performed in 700 m*M* NaCl, 20 m*M* Tris–HCl, pH 7.4. The extinction coefficient of M protein at 280 nm was determined by triplicate amino acid analyses of two independent M preparations of known optical density (at 280 nm). Samples were hydrolyzed for 24 hr under reduced pressure at 110° in constant-boiling HCl containing 1% (w/v) phenol. Analyses were performed on acid hydrolysates with a Beckman 7300 amino acid analyzer using ninhydrin for detection. This method yielded an $\epsilon_{0.1\%}$ value of 1.20 ($\pm$0.01) cm^2/mg at 280 nm. In a second assay, the M protein concentration was determined by titration of its unique cysteine using 5,5′-dithiobis(2-nitrobenzoic acid) (DTNB) which reacts with thiols and generates a thionitrobenzoate ion (TNB^-). About 10 μM M protein with a known optical density at 280 nm was diluted in 6 *M* urea, 20 m*M* Tris–HCl, pH 8, containing 50 μM DTNB. After 15 min of incubation at 20°, the absorbance was measured at 412 nm and the concentration of TNB^- (i.e., the initial cysteine concentration) was determined assuming that the difference of molar absorbance between DTNB and TNB^- is 13,600 M^{-1} cm^{-1}. This yielded an $\epsilon_{0.1\%}$ value of 1.20 ($\pm$0.03) cm^2/mg. Since the values from both assays were the same the M protein concentration was determined by absorbance measurements at 280 nm using the $\epsilon_{0.1\%}$ value of 1.2.

The sedimentation coefficient of M protein was measured by analytical centrifugation as previously described (*24*). Sedimentation of M protein was tested at 0.2, 0.6, and 3.4 mg/ml at 60,000 rpm. Sedimentation coefficients were obtained from linear regression lines where ln *r* was plotted against the sedimentation time (*r* being the distance from the center of the rotor to the sedimenting boundary). We observed monomers with $s_{20°,w} = 2.1 \pm 0.04$ S (see Table 1), independent of the protein concentration. At the highest concentration (3.4 mg/ml), about 20% of the population of particles had an *s* value of about 2.7 S, probably corresponding to dimers.

The diffusion coefficient was measured by dynamic light scattering (DLS). The protein was used at a concentration of 0.5 mg/ml and filtered into the scattering cell through a 50-nm filter (Nucleopore, Pleasanton, U.S.A.). DLS data were collected over an angular range of 25°–90° by the procedure described in (*25*) and analyzed by a double-exponential fit. Two components were sufficient to fit the data at all scattering angles (θ); the major fast component was taken as the contribution from the M protein, while a slower component corresponded to the presence of residual dust or aggregates. The diffusion coefficient of the fast component with relaxation time τ, $D = (K^2\tau)^{-1}$ where *K* is the scattering vector $[K] = (4\pi/\lambda)\sin(\theta/2)$, was independent of the scattering angle. The residual dust contribution did not exceed 20% at the lowest scattering vectors and was below 10% at angles $>45°$.

The diffusion and sedimentation coefficients were corrected to standard conditions to obtain $s_{20°,w}$ and $D_{20°,w}$ values, using solvent densities and viscosities given in the *CRC Handbook of Chemistry and Physics.* Combining the measured *s* and *D* values and assuming a partial specific volume of 0.73 cm^3 g^{-1} for the M protein (calculated from the amino acid sequence) a molecular weight of 31,500 Da can be calculated, close to the value of 26,100 Da obtained from the amino acid sequence. Using relationships ([b]) and ([c]) (legend of Table 1), we calculated the hydrodynamic radius of M protein to be 30 Å (from the sedimentation data) and 36 Å (from the light scattering data; see Table 1), which should be compared with a theoretical R_s of 20 Å for a 26-kDa *globular* protein. The discrepancy between the measured R_s and the theoretical R_s for a globular protein suggests that the shape of VSV M protein is not globular at all, in agreement with the results of McCreedy *et al.* (*13*).

Small-angle neutron scattering was measured on the instrument D11 (*26, 27*) at the high-flux reactor of the Institut Laue-Langevin in Grenoble, France. Data were measured in two instrumental configurations: (i) sample-detector distance of 1.5 m, incident neutron wavelength 6 Å giving a range of scattering vectors, *Q* ($Q = (4\pi/\lambda)\sin\theta$; 2θ = scattering angle) from 0.035 to 0.24 Å^{-1} and (ii) sample-detector distance of 5 m, incident neutron wavelength 10 Å, giving $0.006 < Q < 0.046$ Å^{-1}. Neutron scattering from the protein alone was measured by subtracting the scattering by the buffer from that by the protein solution. The data were placed on an absolute scale and corrected for differential spatial response of the detector by normalizing to the scattering of a 1-mm-thick sample of water. Samples were contained in quartz cuvettes (Hellma, France) having a pathlength of 1 mm and a surface area exposed to the neutron beam of 70 mm^2. Protein concentrations were measured by UV spectroscopy in the same cuvettes as for the neutron-scattering measurements. The lowest scattering angle data of a neutron-scattering experiment are shown in Fig. 1A as a Guinier plot. From the slope of the line fitted through the data points we can obtain the radius of gyration (R_g, defined by the relationship $MR_g^2 = \int r^2 dm$ where *r* is the distance of the element of mass *dm* from the mass center of the molecule and *M* is the molecular weight of the molecule) of the protein and from the extrapolation to $Q = 0$ we obtain the zero angle intensity $I(0)$ which, when normalized to the protein concentration, yields the protein molecular weight (*28*). From this analysis we ob-

TABLE 1

Hydrodynamic Parameters of VSV M Protein

Parameters	Sedimentation coefficient (S)	Diffusion coefficient (10^{-11} m^2/sec)	Radius of gyration (Å)
Value	$s_{20,w} = 2.1 \pm 0.04$	$D_{20,w} = 5.89 \pm 0.1$	$R_g = 28.9 \pm 2.7$ R_g section $= 6.9 \pm 0.1$
Technique	Analytical centrifugation	Light scattering	Neutron scattering
Derived R_s[a]	30 Å[b]	36 Å[c]	32 Å[d] and 30 Å[e]

[a] For all measured parameters, a corresponding hydrodynamic radius (R_s) was calculated according to formulas specified below ([b] to [d]). R_s corresponds to the radius of a sphere that presents the same frictional coefficient as that of the molecule. For a spherical molecule, R_s is equal to the radius of the molecule.

[b] $R_s = M(1 - \rho v)/6\pi\eta N_A s$ where M is the molecular weight, ρ the density, η the viscosity of the medium, v the partial specific volume, N_A Avogadro's number, and s the sedimentation coefficient.

[c] $R_s = k_B T/6\pi\eta D$ where k_B is the Boltzmann's constant and T the absolute temperature.

[d] and [e] Calculated according to a cylindrical model of half-length a and radius b with $R_s = a/\ln(a/b + \gamma)$; γ is an end effect correction and is approximately 0.4 for the range of the axial ratios considered here. In ([d]), a and b were calculated from $R_g^2 = a^2/3 + b^2/2$ and the volume of the M protein $V_M = \pi b^2 2a$. In ([e]) a and b were calculated from R_g section $= b/\sqrt{2}$ and V_M.

tained an R_g of 29 ± 3 Å and a molecular weight of 33.6 ± 4 kDa. Again, these results should be compared to the radius of gyration of a spherical protein with a mass of 26 kDa which would be about 15 Å. The high molecular weight can be partly explained by the presence of dimers that were also observed at high protein concentrations in the sedimentation experiments.

The higher angle data are shown in Fig. 1B, where we plotted the data in a different manner from that in Fig. 1A (see legend). This way of plotting should show the data points on a straight line if the sample has the shape of a rod (*29*) where the slope of the line should give the radius of gyration of the cross-section of the rod (R_c). The results shown in Fig. 1B indeed suggest that M protein has a rod shape with an R_c of 6.9 ± 0.1 Å, which corresponds to radius of about 10 Å ($=\sqrt{2}R_c$) if the rod has a circular cross-section. Attempts to fit the data to a thin disk led to unrealistic models.

The radius of gyration of a cylinder is given by $R_g^2 = a^2/3 + b^2/2$, where a is the half-length and b the cross-sectional radius. Assuming a circular cross-section for the molecule with a radius (b) of 10 Å (see above), we can calculate the length of the rod: 98 Å. Thus, the neutron-scattering experiments would suggest that VSV M protein is a thin rod with a width of some 20 Å and a length of about 100 Å. When these values are used to calculate a hydrodynamic radius (R_s) we obtain about 30–32 Å (see Table 1), which is in excellent agreement with the estimates from the sedimentation experiments but somewhat lower than calculated from the light-scattering experiment. We have tried to observe the M protein with negative-stain and metal-shadowing electron microscopy. Although we sometimes did observe thin elongated molecules with the diameters above, the results were never convincing, probably because the proposed width of M protein is too close to the resolution limit of these

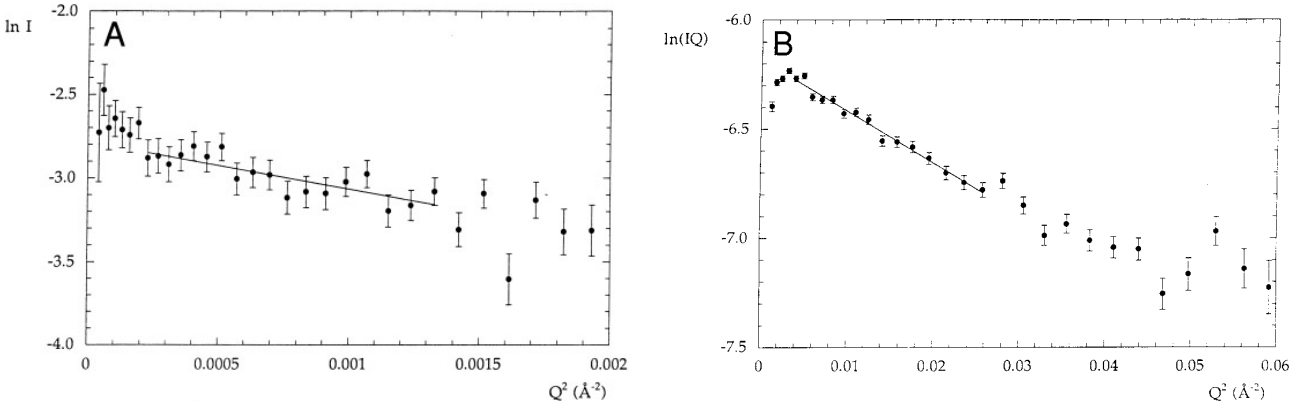

FIG. 1. Small-angle neutron scattering curves of M protein. (A) At lowest angles, the data are plotted in the form of a Guinier plot (*45*), i.e., ln $I(Q)$ vs Q^2 where I is the intensity and Q the scattering vector (see text). (B) At higher angles, the data are plotted as $\ln[I(Q)Q]$ vs Q^2. See text for further explanation. In both cases, the data points used in the calculations were those connected by the straight lines.

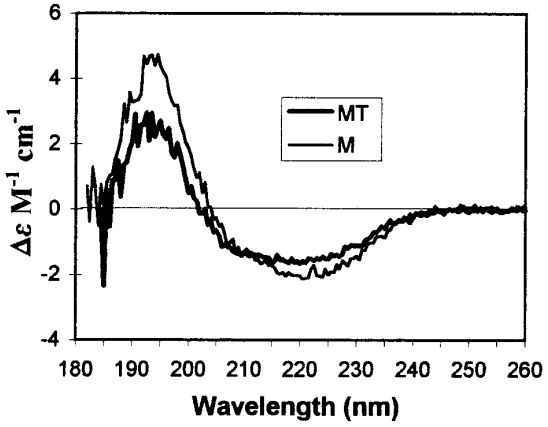

FIG. 2. Far-UV CD spectrum of the isolated M protein (thin line) and MT protein (bold line). In order to obtain MT (*24, 46, 47*), M protein (in 700 m*M* NaF, 10 m*M* phosphate, pH 7.4) was digested by biotinylated trypsin (Sigma; weight ratio 1/5). Biotinylated trypsin was then removed on an avidin–Sepharose column. The spectra were measured with a Jobin Yvon CD6 dichrograph at 25° with a 1-mm (resp. 2 mm) pathlength sample cell for M (resp. MT). Each spectrum was the result of averaging 10 successive spectra. Before analysis, the proteins were spun in an Airfuge (5 min, 30 psi) to remove potential aggregates. M concentration was 25.6 μg/ml and MT concentration was 16.5 μg/ml. $\Delta\epsilon$, differential molar extinction coefficient (per residue).

techniques and possibly also because the M protein may be somewhat flexible or may adopt various conformations when it is adsorbed onto the EM grids. Previous electron microscopy work on the "cigar-like" structure inside the virion and on aggregates of M (*18, 24*) suggested that both structures consist of fine filaments with a width of about 20 Å, corresponding to the width of M protein derived here. The present results are in agreement with the idea that the "cigar" structure observed inside the virus particle consists indeed of M protein.

Far-UV circular dichroism was then used to identify the secondary structure content of M protein. The far-UV CD spectra of M protein (extensively dialyzed against 700 m*M* NaF, 10 m*M* phosphate, pH 7.4) and its 21-kDa tryptic-resistant core (MT) were recorded and analyzed. Figure 2 shows the spectra of M (between 182 and 260 nm) and MT (between 184.5 and 260 nm) after substracting the contribution of the buffer. Deconvolution of the spectrum for M protein by the variable selection (VARSELEC) method of Hennessey and Johnson (*30, 31*) indicated an α-helix content of about 24%, whereas analysis by the method of Chang and colleagues (*32, 33*) suggested an α-helical content of about 41%. This discrepancy could be due to the presence of very short α-helices (less than 6 residues) which have a different spectrum from the long helices (the algorithm of Chang *et al.* takes the length of the helix into account). Analysis of the spectrum of MT protein gave values of 19 and 34% (for the analysis methods of Hennessey and Johnson and Chang *et al.,* respectively), indicating that the amino-terminal peptide (1–43) removed by trypsin may be partly helical. Both programs also suggested the presence of β-strands.

In principle, a long thin molecule could consist of an antiparallel double α-helical coiled coil. Considering the possibility that such a structure could have loops at both ends contributing to the length, the α-helical content derived from the CD measurements, especially the 41% calculated from the Chang *et al.* (*32, 33*) analysis, does not necessarily exclude this potential structure. We, therefore, decided to investigate secondary structure predictions of M protein. The amino acid sequences of the matrix proteins of four vesiculoviruses were aligned by hand as shown in Fig. 3. Three different methods were used to predict the secondary structures of the four matrix proteins: The Chou and Fasman algorithm (CF) (*34–36*), the Garnier Robson algorithm (GR) (*37*), and the secondary structure prediction program on the PHD PredictProtein server at EMBL Heidelberg (RS) (*38–40*). In Fig. 3, we have outlined the regions for which all three methods predict α-helices or β-strands in at least three of the four proteins. Two regions extending from aa 60 to aa 116 (VSV-Ind numbering) and from aa 170 to the C-terminus of the molecule were predicted to be rather rich in secondary structure, whereas the region extending from aa 116 to 169 and the amino-terminal part of the molecule, which have a high proline content, were predicted to be coil and turn.

The amino-terminal part of the protein is hydrophilic and corresponds to the fragment of the protein which is removed by trypsin cleavage after K43, suggesting "independence" from the rest of the M protein. All programs predict an α-helix at the amino-terminal extremity of the protein but with varying length depending on the program and on the specific sequence. In fact, the comparison of the CD spectra of M and MT would suggest that more than 6 residues between the amino-terminus and K43 are in an α-helical conformation. An increasing body of evidence suggests that this domain is involved in the interaction between the matrix protein and the cell membrane. Using ^{125}I-TID, a hydrophobic photoactivatable reagent, Lenard and Vanderoef (*23*) have suggested that the amino-terminal part of M penetrates the bilayer. This is consistent with the recent results of Chong and Rose (*11*) who have shown that the 16 amino-terminal amino acids were necessary for stable interaction between M and the plasma membrane. The amphiphilicity of the aminoterminal α-helix may indicate that it can lie at the surface of the cell membrane, its hydrophobic side penetrating the membrane.

The secondary structure analysis of vesiculovirus M protein was combined with additional sequence information on the M proteins of rabies, Mokola, and Sigma virus (*41–43*). Although the sequences of these other

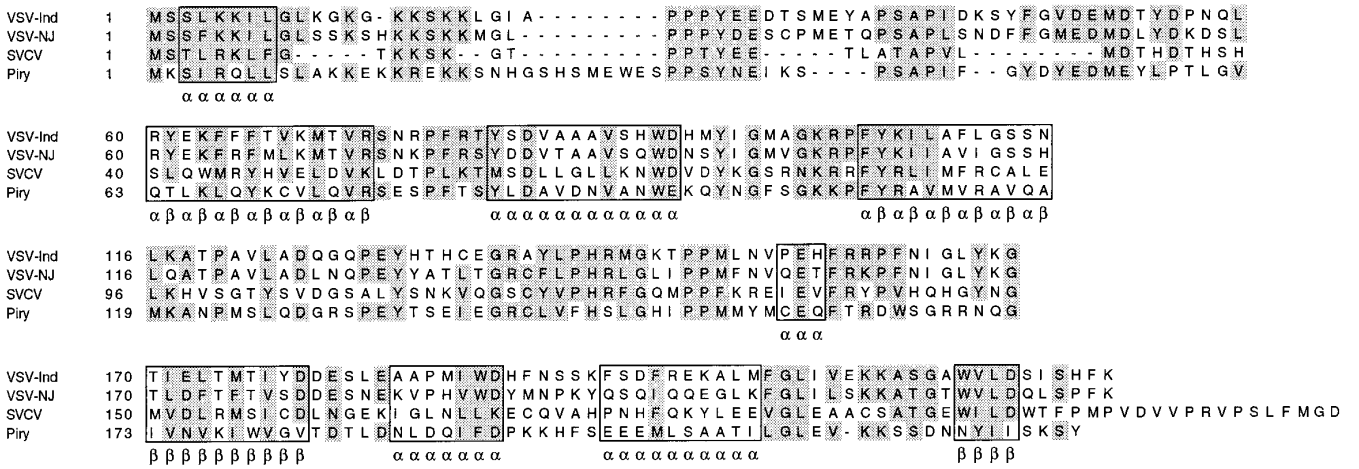

FIG. 3. Sequence alignment and secondary structure prediction of four vesiculoviruses: VSV Indiana (VSV-Ind; *48*), VSV New Jersey (VSV-NJ; *49*), spring viremia of carp virus (SVCV; *50*) and Piry virus (access code for Genbank database PVPPMG.PE2). Shaded residues are conserved or show conservative changes. Outlined sequence is predicted by all three secondary structure prediction methods to contain the structure as indicated below the sequence (α for helix and β for strand). The sequences that are indicated by $\alpha\beta\alpha\beta$ are strongly predicted by all three methods to contain secondary structure, but by one to be helical and by another to be β-strand.

rhabdovirus M proteins can be aligned with the vesiculovirus M proteins (*43*), they show such poor homology that they are not found in a database by an automatic homology search with VSV M protein. However, the alignment of Bras *et al.* (*43*) indicates the presence of important insertions and deletions in the rhabdovirus M proteins in the region corresponding to aa 116–169 (VSV Indiana numbering). This, together with the absence of predicted strand and helix in this region, suggests that this part of the protein consists of variable loops (*44*).

In general, it appears that those regions that are most strongly predicted to be coil or turn, the proline-rich stretches in the amino-terminal region, and the connecting sequences between predicted α-helix and β-sheet are among the best conserved. The residues predicted by both CF and GR to be in α-helical conformation amount to 32% of the sequence, those predicted by the RS method to 29%, in between the values calculated by the CD analysis methods of Hennessey and Johnson (*30, 31*) and Chang *et al.* (*32, 33*). The sequence of M protein does not contain heptad repeats, a prerequisite for coiled coils, and the secondary structure predictions suggest that VSV M protein does not contain enough helix to form a double-coiled coil.

To conclude, we would like to stress that this study was performed on the soluble matrix protein isolated from virus. As mentioned above, it is supposed that there exist two different populations of M protein; one which is soluble and the other which has the characteristics of an integral membrane protein. It is possible that, in the hydrophobic environment of the membrane, the structure of M protein is different from that of soluble, monomeric M protein and that, perhaps, the $\alpha\beta\alpha\beta$ regions (which are strongly predicted by all three methods to contain secondary structure, but by one to be helical and by another to be β-strand) adopt different conformations in the two types of M protein.

ACKNOWLEDGMENTS

We thank Christine Ebel for support with the analytical centrifugation experiments and helpful discussions and Stephen Cusack for critical comments and ideas.

REFERENCES

1. Carroll, A. R., and Wagner, R. R., *J. Virol.* 29, 134–142 (1979).
2. De, B. P., Thornton, G. B., Luk, D., and Banerjee, A. K., *Proc. Natl. Acad. Sci. USA* 79, 7137–7141 (1982).
3. Clinton, G. M., Little, S. P., Hagen, F. S., and Huang, A. S., *Cell* 15, 1455–1462 (1978).
4. Martinet, C., Combard, A., Printz-Ane, C., and Printz, P., *J. Virol.* 29, 123–133 (1979).
5. Blondel, D., Harmison, G. G., and Schubert, M., *J. Virol.* 64, 1716–1725 (1990).
6. Melki, R., Gaudin, Y., and Blondel, D., *Virology* 202, 339–347 (1994).
7. Black, B. L., and Lyles, D., *J. Virol.* 66, 4058–4064 (1992).
8. Black, B. L., Rhodes, R. B., McKenzie, M., and Lyles, D. S., *J. Virol.* 67, 4814–4821 (1993).
9. Bergmann, J. E., and Fusco, P. J., *J. Cell Biol.* 107, 1707–1715 (1988).
10. Chong, L. D., and Rose, J. K., *J. Virol.* 67, 407–414 (1993).
11. Chong, L. D., and Rose, J. K., *J. Virol.* 68, 441–447 (1994).
12. Ye, Z., Sun, W., Suryanarayana, K., Justice, P., Robinson, D., and Wagner, R., *J. Virol.* 68, 7386–7396 (1994).
13. McCreedy, B. J., Jr., McKinnon, K. P., and Lyles, D. S., *J. Virol.* 64, 902–906 (1990).
14. Knipe, D. M., Baltimore, D., and Lodish, H. F., *J. Virol.* 21, 1128–1139 (1977).
15. Newcomb, W. W., and Brown, J. C., *J. Virol.* 39, 295–299 (1981).
16. Newcomb, W. W., Tobin, G. J., McGowan, J. J., and Brown, J. C., *J. Virol.* 41, 1055–1062 (1982).
17. Odenwald, W. F., Arnheiter, H., Dubois-Dalcq, M., and Lazzarini, R. A., *J. Virol.* 57, 922–932 (1986).

18. Barge, A., Gaudin, Y., Coulon, P., and Ruigrok, R. W. H., *J. Virol.* 67, 7246–7253 (1993).
19. Zakowski, J. J., and Wagner, R. R., *J. Virol.* 36, 93–102 (1980).
20. Zakowski, J. J., Petri, W. A., Jr., and Wagner, R. R., *Biochemistry* 20, 3902–3907 (1981).
21. Pal, R., Barenholz, Y., and Wagner, R. R., *Biochim. Biophys. Acta* 906, 175–193 (1987).
22. Brown, J. C., and Newcomb, W. W., *In* "Animal Virus Structure" (M. V. Nermut and A. C. Steven, Eds.), pp. 199–212. Elsevier, Amsterdam, 1987.
23. Lenard, J., and Vanderoef, R., *J. Virol.* 64, 3486–3491 (1990).
24. Gaudin, Y., Barge, A., Ebel, C., and Ruigrok, R. W. H., *Virology* 206, 28–37 (1995).
25. Krueger, S., Zaccai, G., Wlodawer, A., Langowski, J., O'Dea, M., Maxwell, A., and Gellert, M., *J. Mol. Biol.* 211, 211–220 (1990).
26. Ibel, K., *J. Appl. Crystallogr.* 9, 296–309 (1976).
27. Lindner, P., May, R., and Timmins, P. A., *Physica B* 180 & 181, 967–972 (1992).
28. Jacrot, B., and Zaccai, G., *Biopolymers* 20, 2413–2426 (1982).
29. Luzatti, V., *Acta Crystallogr.* 13, 939–945 (1960).
30. Hennessey, J. P., Jr., and Johnson, W. C., Jr., *Biochemistry* 20, 1085–1094 (1981).
31. Manavalan, P., and Johnson, W. C., Jr., *Anal. Biochem.* 167, 76–85 (1987).
32. Chang, C. T., Wu, C.-S. C., and Yang, J. T., *Anal. Biochem.* 91, 12–31 (1978).
33. Yang, J. T., Wu, C.-S. C., Martinez, H. M., *Methods Enzymol.* 130, 208–269 (1986).
34. Chou, P. Y., and Fasman, G. D., *Biochemistry* 13, 211–222 (1974).
35. Chou, P. Y., and Fasman, G. D., *Biochemistry* 13, 222–245 (1974).
36. Chou, P. Y., and Fasman, G. D., *J. Mol. Biol.* 115, 135–175 (1977).
37. Garnier, J., Osguthorpe, D. J., and Robson, B., *J. Mol. Biol.* 120, 97–120 (1978).
38. Rost, B., and Sander, C., *J. Mol. Biol.* 232, 584–599 (1993).
39. Rost, B., and Sander, C., *Cabios* 10, 53–60 (1994).
40. Rost, B., and Sander, C., *Proteins* 19, 55–72 (1994).
41. Rayssiguier, C., Cioe, L., Withers, E., Wunner, W. H., and Curtis, P. J., *Virus Res.* 5, 177–190 (1986).
42. Bourhy, H., Kissi, B., and Tordo, N., *Virology* 194, 70–81 (1993).
43. Bras, F., Teninges, D., and Dezelee, S., *Virology* 200, 189–199 (1994).
44. Barton, G. J., *Curr. Opinion Struct. Biol.* 5, 372–376 (1995).
45. Guinier, A., and Fournet, G., "Small Angle Scattering of X-Rays." Wiley, New York, 1955.
46. Pal, R., Grinnell, B. W., R. M., Wiener, J. R., Volk, W. A., and Wagner, R. R., *J. Virol.* 55, 298–306 (1985).
47. Kaptur, P. E., Rhodes, R. B., and Lyles, D. S., *J. Virol.* 65, 1057–1065 (1991).
48. Rose, J. K., and Gallione, C. J., *J. Virol.* 39, 519–528 (1981).
49. Gill, D. S., and Banerjee, A. K., *Virology* 150, 308–312 (1986).
50. Kuichi, A., and Roy, P., *Virology* 134, 238–243 (1984).